ACS OMEGA

http://pubs.acs.org/journal/acsodf

Article

Synthesis of Si−Ge Nanosheets and Their Dispersion of Organic Solvents with Focus on the Hansen Solubility Parameters

Hideyuki Nakano*,# and Daisuke Nakamura*,#

Cite This: *ACS Omega* 2022, 7, 18834−18839

Read Online

ACCESS | Metrics & More | Article Recommendations | Supporting Information

ABSTRACT: Two-dimensional (2D) materials combine the collective advantages of individual building blocks and synergistic properties and have spurred great interest as a new paradigm in materials science. Especially, exfoliation of 2D semiconductive materials into nanosheets is of significance for both fundamental and potential applications. In this report, silicon−germanium (Si−Ge) nanosheets were synthesized by sonication of porous Si−Ge powder. The raw material Si−Ge powder was obtained by leaching Li from $Li_{13}Si_2Ge_2$ with ethanol; after that, it was crystallized by heat treatment at 500 °C. The thickness and the lateral size of the exfoliated Si−Ge nanosheets were about 3 nm and a few microns, respectively. The nanosheets were dispersed in 55 different organic solvents, and their Hansen solubility parameters were calculated and compared with those of the end member (Si and Ge) nanosheets and graphene.

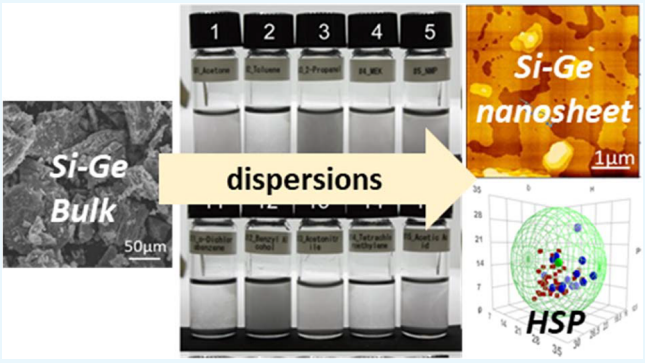

INTRODUCTION

Silicon−germanium (Si−Ge) is an alloy that can have any proportion of its constituent elements and has the chemical formula $Si_{1-x}Ge_x$. Among various applications, it has been used in integrated circuits and heterojunction bipolar transistors as a semiconductor material and in complementary metal oxide semiconductors (CMOSs) as a strain-inducing layer material. $Si_{1-x}Ge_x$ has also been used as a thermoelectric material in high-temperature applications and can be fabricated on Si wafers via conventional Si processing methods.[1−3] Therefore, $Si_{1-x}Ge_x$ can be fabricated at costs similar to those of Si CMOS manufacturing, which are lower than the costs associated with other heterojunction technologies (e.g., GaAs).

Organogermanium precursors such as isobutylgermane, alkylgermanium trichlorides, and dimethylaminogermanium trichloride have been investigated as less hazardous liquid alternatives to germanium hydrides for depositing Ge-containing films (e.g., films of high-purity Ge, Si−Ge, and strained Si) via metal−organic vapor-phase epitaxy.[4] However, monolayers of Si and Ge as well as those of chalcogenide compounds and graphene have been active research topics.

We have been studying the exfoliation and functionalization of layered Si compounds in the liquid phase and have been successful in the derivatization of various silicon nanosheets (SiNSs) from layered silicon compounds.[5−8] The resulting sheet has a structure in which organic groups are attached to the top and bottom of one layer of the silicon (111) plane, and the lateral size is on the microscale. For example, the thickness of the sheet terminated with a hydroxyl group is ca. 0.3 nm,[9] and when a phenyl group is added, the thickness is ca. 1 nm.[10] Recently, we have derived Si and GeH nanosheets from $Li_{13}Si_4$ and layered germanene GeH, respectively,[11,12] and the model structure of the obtained sheets is shown in Scheme 1. The Si nanosheet has the same structure as diamond-type Si, with a thickness of ca. 4 nm and a lateral size on the microscale. On the other hand, a GeH nanosheet has a Ge monoatomic layer with the same atomic arrangement as the germanium (111) plane of a diamond

Scheme 1. Schematic Describing the Synthesis and Dispersion of (a) GeH Nanosheets and (b) Si and/or Si−Ge Nanosheets

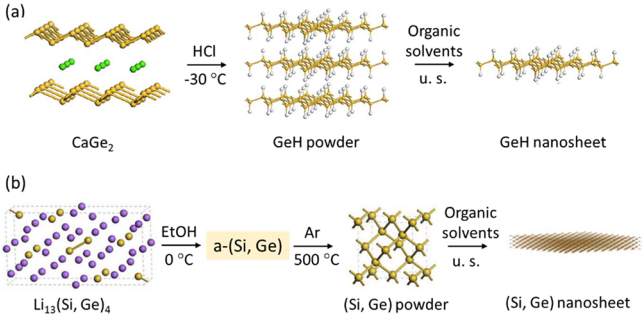

Received: March 24, 2022
Accepted: May 11, 2022
Published: May 23, 2022

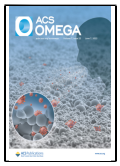

https://doi.org/10.1021/acsomega.2c01776
ACS Omega 2022, 7, 18834−18839

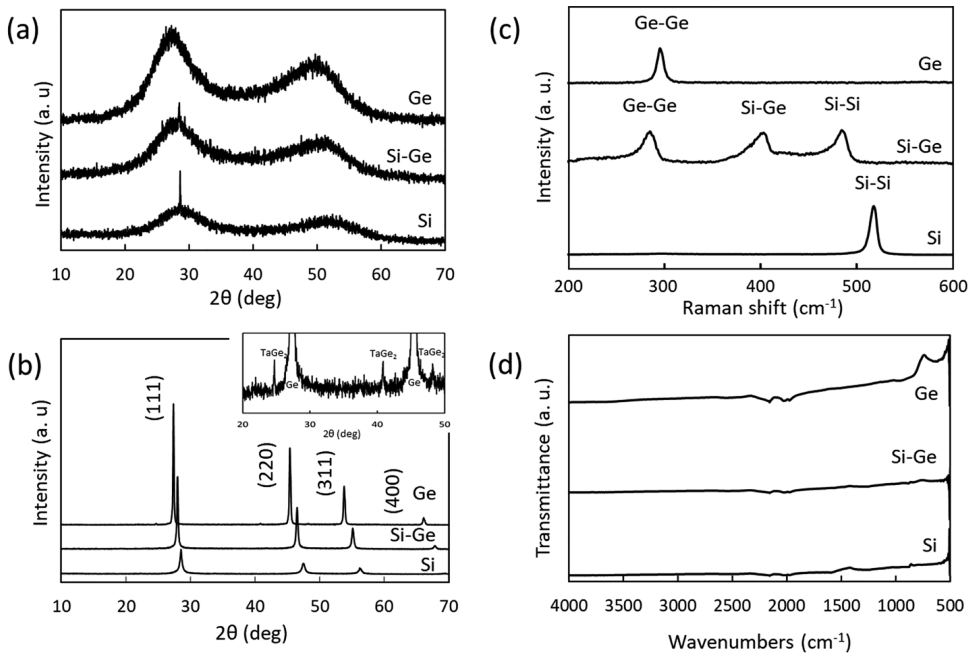

Figure 1. XRD patterns for porous Si, Si−Ge, and Ge: (a) as-prepared samples, (b) samples after heating at 500 °C under argon for 1 h (inset; enlarged XRD pattern of Ge), (c) Raman spectra and (d) FTIR spectra of (b). In the FTIR spectra, the slight baseline distortion at 2000−2300 cm^{-1} is caused by the strong background absorption of the diamond ATR crystal.

structure, with hydrogen terminations on the top and bottom. The thickness of the obtained sheet was ca. 3 nm (equivalent to about 10 GeH layers), and the lateral size is on the microscale, as for SiNS. Since these sheets are expected to be applied to semiconductor devices, it is necessary to produce ink in which the sheets are dispersed with high yield. To solve this problem, our group has been using Hansen solubility parameters (HSPs) to design such inks with well-dispersed GeH sheets.[11−14] HSPs classify solvent−solvent interactions into dispersive, polar, and hydrogen-bonding components. These components, in conjunction with an interaction value, are also used to describe solute. Although additional parameters can be used, these three components tend to provide reliable results.[15] Whereas the Hildebrand solubility is sufficient for developing ink formulations of nonpolar substances, the surface chemistry of capped nanoparticles usually necessitates that polar and hydrogen-bonding components be considered in the development of nanoparticle-based inks.[16,17]

In this study, Si−Ge nanosheets were synthesized from $Li_{13}Si_2Ge_2$ and the dispersion properties of the obtained sheets were evaluated using their HSPs.[18−21] We also compared the HSPs of the obtained nanosheets with those previously reported for Si and Ge nanosheets.

METHODS

Synthesis of Si, Ge, and Si−Ge Nanosheets. According to the previously reported method shown in Scheme 1b,[11,22] Si, Ge, and Si−Ge nanosheets were synthesized by etching $Li_{13}Si_4$, $Li_{13}Ge_4$, and $Li_{13}Si_2Ge_2$ alloys with ethyl alcohol, respectively. Li alloys were prepared by radiofrequency heating of Li, Si, and Ge pieces. Thereafter, the alloys (1 g) were reacted with ethyl alcohol (500 mL) and cooled at 0 °C to remove Li. The mixture was stirred for 120 min at 0 °C, and the mixtures were filtered. The remaining powder was added to acetic acid (200 mL) and was stirred for 60 min at r.t. The filtered powders were dried at 100 °C in vacuum for 120 min. To crystallize the sample, the as-prepared powder was heated under Ar at 500 °C for 1 h. The obtained sample was confirmed to be free of Li salt (Li_2CO_3) by IR measurements.

Dispersion in Organic Solvents. The Si−Ge powder (5 mg) was charged into 4 mL vials that were individually filled with 2 mL of probe liquid, according to a previously reported method.[11,12] There were a total of 55 probe liquids used, which were rationally chosen to cover a wide variety of molecular interactions in terms of HSPs. The vials containing the silicon nanosheet source powder and probe liquids were sonicated for 10 min in an ultrasonic bath and then photographed after 2 h, 1 day, and 2 days of sedimentation to monitor dispersion stability. The intensities of light (divided into three primary colors of red (R), green (G), and blue (B)) transmitted through the dispersions (I_{RD}, I_{GD}, and I_{BD}, respectively) as well as the background light intensity (I_{RB}, I_{GB}, and I_{BB}, respectively) were extracted from the image data for the dispersions. The apparent light transmittance T of the dispersions was then calculated using the following equation:

$$T = \frac{I_{RD} + I_{GD} + I_{BD}}{I_{RB} + I_{GB} + I_{BB}} \quad (1)$$

T can be transformed to the absorbance per unit length (A/l), which directly correlates to the concentration of nanosheets dispersed in the probe liquids.

In this study, it is assumed that the light transmittance T is inversely correlated with the exfoliated nanosheet concentration in the dispersion. For the calculation of the HSP values, the solvents were ranked "good" and "bad" with marks ranging from 1 (good) to 4 (very poor). The center of this sphere has also a set of HSPs and could be used in combination with the database to find suitable solvents for the nanosheets. In the present study, probe liquids with T < 60% (2 h of sedimentation), 80% (1 day of sedimentation), and 85% (2 days of sedimentation) for the exfoliation and dispersion of the Si−Ge nanosheets were deemed as good solvents.

https://doi.org/10.1021/acsomega.2c01776
ACS Omega 2022, 7, 18834−18839

The HSP is one of the indicators for molecular interactions. It is an effective tool to predict and/or examine the compatibility (e.g., dispersibility, solubility, and wettability) of two different materials. The HSP consists of three terms that originate from corresponding molecular interactions: δD (London dispersion term), δP (polar term), and δH (hydrogen bonding term). The compatibility of two different materials (with respective HSPs of $[\delta D_1, \delta P_1, \delta H_1]$ and $[\delta D_2, \delta P_2, \delta H_2]$) can be estimated by the HSP distance R_a, which is defined as follows:

$$R_a = \sqrt{4 \times (\delta D_1 - \delta D_2)^2 + (\delta P_1 - \delta P_2)^2 + (\delta H_1 - \delta H_2)^2} \quad (2)$$

A small R_a value indicates better compatibility of two different materials. Because the HSPs for typical organic solvents are already known, the HSPs for the probe liquids used in this study were obtained from the official HSP database and are listed in Table S1.[18] In addition, the radius of the HSP sphere is referred to as the interaction radius R_0, which is a tolerance indicator of a new material to interact with other materials. This, however, depends on how stringent the qualification criteria for a good solvent are chosen.

RESULTS AND DISCUSSION

Characterization of the Nanosheets. Similar to the previously reported Si nanosheet derived from $Li_{13}Si_4$,[11,22] $Li_{13}Si_2Ge_2$ in ethyl alcohol resulted in black precipitation with hydrogen generation. The X-ray diffraction (XRD) patterns for bulk Si−Ge powder together with that for Si and Ge powders prepared from $Li_{13}Si_4$ and $Li_{13}Ge_4$ are shown in Figure 1. The bulk samples after ethanol treatment were amorphous, giving a broad halo in all systems. Although a small amount of Si that did not react with Li during preparation of Li−(Si, Ge) alloys remained in the Si and Si−Ge powders (Figure 1a), all samples became crystalline when heated at 500 °C under argon as shown in Figure 1b. The peaks for the Si and Ge powders were assigned to a diamond-type structure. In this study, peaks due to Si−Ge are observed between those of Si and Ge, indicating that Si−Ge is a solid solution of the end member. A small amount of $TaGe_2$ is observed in the enlarged image of the Ge nanosheet in Figure 1b; it has been reported that a small amount of $TaSi_2$ is formed when the Ta crucible is reused during the synthesis of $CaSi_2$.[23] In this study, because the same Ta crucible was used for the synthesis of $Li_{13}Ge_4$ and $LiSi_2Ge_2$, a small amount of $TaGe_2$ is thought to have been generated as a byproduct during the synthesis of $Li_{13}Ge_4$. To evaluate the long-term stability of the nanosheets, XRD measurements were performed on samples dispersed in the solvent for 2 days and for 4 months. After 2 days, the exfoliated nanosheets retained their crystal structure. However, after 4 months of dispersion in the atmosphere, the crystalline Si sheets had become amorphous. XRD patterns for a sample dispersed and stored in ethyl alcohol and DMSO, respectively, are shown in Figure S1. This result may be explained by the slow reactivity of oxygen with the sheet surface. Raman spectroscopy has been used to characterize the strain and composition of $Si_{1-x}Ge_x$ dots grown on Si substrates via various methods such as MBE and CVD.[24−26] Si and Ge crystallize in the same structure as diamond and comprise two interpenetrating face-centered cubic lattices, which yields a single triply degenerate optical vibration mode at zero wavevector at 520 cm^{-1} for Si and 300 cm^{-1} for Ge at room temperature (Figure 1c). The Raman spectrum of this Si−Ge material shows three main peaks: the Ge−Ge (286 cm^{-1}), Si−Ge (405 cm^{-1}), and Si−Si (486 cm^{-1}) vibrational modes (Figure 1c). Shin *et al.* reported that in the $Si_{1-x}Ge_x$ alloy system, the Si−Si and Ge−Ge mode frequencies as functions of x are best fitted with a linear function, while the Si−Ge mode is best fitted with a fourth-order polynomial.[24] That is, the Si−Si (Ge−Ge) mode frequency decreases (increases) with x, while the Si−Ge mode frequency increases for $x \leq 0.56$ and decreases for $x > 0.56$. According to the previous report, the composition of the present Si−Ge sample was calculated to be $Si_{0.52}Ge_{0.48}$, which was in good agreement with the prepared composition. In the reaction system, the removed Li exists as LiOH, which is considered to be Li_2CO_3 when exposed to the atmosphere. As no −OH (~3000 cm^{-1}) or $-CO_3$ (~1700 cm^{-1}) groups were observed in Figure 1d, it was concluded that no Li remained in the sample.

In Figure 2a,b, particles with a diameter of ~20 to ~50 μm are observed, which have an interior that formed a layered structure.

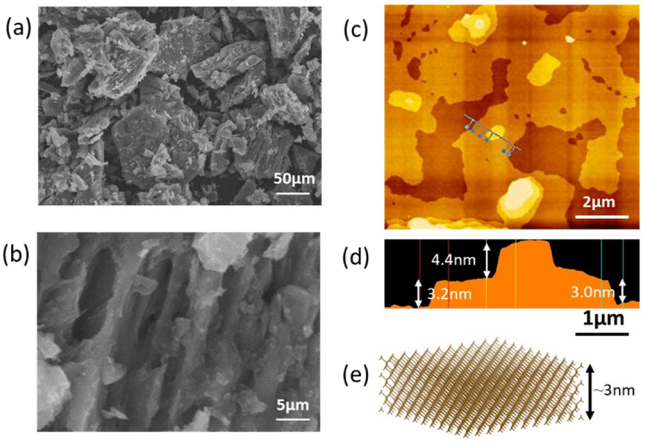

Figure 2. (a) Scanning electron microscopy (SEM) and (b) enlarged SEM images of Si−Ge crystalline powder. (c) AFM image of Si−Ge nanosheet. (d) Line profile taken along the blue line in (c). (e) Schematic model of Si−Ge nanosheet.

The Si−Ge powder was ultrasonicated in ethanol for 30 min and centrifuged at 13,000 rpm for 3 min, corresponding to a relative centrifugal acceleration of 40,000 at the cell bottom. Then, the supernatant liquid was spin coated onto a Si substrate at 1000 rpm for 30 s for atomic force microscopy (AFM) evaluation. As shown Figure 2c,d, sheets consisting of about 10 Si−Ge layers were observed with a width of several micrometers and a thickness of about 3 nm with a flat surface. This value is almost the same as that for Si and Ge nanosheets.[11,12] In our experiments, the delithiation process produces layered structures with apparent anisotropy. This anisotropy might be related to the crystallographic structure of $Li_{13}Si_2Ge_2$ and associated energy barriers for the Li ion reaction and diffusion (or lithium ionic mobility). Wu *et al.* conducted theoretical considerations, reporting that nanosheet formation is induced by stress due to delithium from $Li_{13}Si_2Ge_2$.[22]

Dispersions of Si−Ge Nanosheets. The stability of Si−Ge nanosheets was qualitatively evaluated by noting which solvents achieved stable dispersions versus those in which the nanosheets agglomerated and precipitated over the time of the experiment. Immediately after sonication, Si−Ge crystalline samples were dispersed into 55 different probes as shown in Table S1, and each parameter of HSP was determined.

https://doi.org/10.1021/acsomega.2c01776
ACS Omega 2022, 7, 18834−18839

Figure 3. Si−Ge nanosheet dispersions in 55 different probe liquids after 2 h of sedimentation.

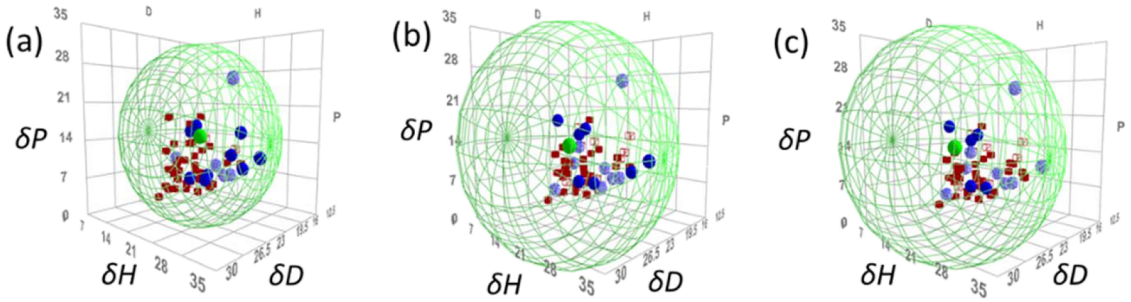

Figure 4. HSP plots of good and poor solvents for Si−Ge nanosheet dispersions, which are determined by the transmittance values of the dispersions after exfoliation and sedimentation experiments conducted for (a) 2 h, (b) 1 day, and (c) 2 days.

Table 1. Comparison of the HSPs Obtained for the Si−Ge, Si, and Ge Nanosheets after Different Sedimentation Times[a]

	HSP [(J/cm^3)$^{1/2}$]						
sample	δD	δP	δH	R_0	FIT	remark	ref
Si-Ge nanosheet #1	23.1	15.4	19.6	15.9	0.63	G/T = 14/55	this work
Si-Ge nanosheet #2	25.8	14.7	19.5	19.9	0.44	G/T = 15/55	
Si-Ge nanosheet #3	26.2	15.3	18.6	19.9	0.47	G/T = 13/55	
Si nanosheet #1	20.4	15.9	14.1	13.0	0.34	G/T = 32/55	([11])
Si nanosheet #2	23.8	18.7	14.1	17.1	0.45	G/T = 18/55	
Si nanosheet #3	26.0	16.7	17.9	19.9	0.48	G/T = 13/55	
GeH nanosheet #1	23.2	14.6	13.9	17.9	0.53	G/T = 19/34	([12])
GeH nanosheet #2	24.7	11.2	17.7	17.9	0.51	G/T = 10/34	
graphene	20.0	11.2	7.3	6.7	1	G/T = 5/12	([19])

[a]FIT values indicate the quality of sphere fitting (FIT = 1 means perfect fitting without anomalies). G/T values indicate the number of good solvents/that of total probe liquids.

Figure 3 and Figures S1 and S2 are the Si−Ge dispersions in the probe solution after 10 min of sonication and subsequent sedimentation (2 h, 1 day, and 2 days). After 2 h, however, dimethyl sulfoxide (DMSO in Figure 3, No. 31) and alcohols gave little to no sediment. After 2 days, a decrease in concentration and eventual sedimentation in the alcohol solutions were observed and Si−Ge dispersions in DMSO exhibited high stability. The raw data for the apparent intensity of light transmitted through the Si−Ge dispersions and the background light apparent intensity were obtained from the image data in Figure 3 and Figures S1 and S2, and the results are summarized in Tables S2−S4. The T values were calculated using eq 1.

Using the transmittance values for the dispersions after the exfoliation and sedimentation experiments (2 h, 1 day, and 2 days), HSP spheres and their center values are plotted as shown in Figure 4, which are depicted by green spheres and green solid circles, respectively. The good solvents inside and outside the HSP sphere are plotted as blue solid circles and blue open circles, respectively, and the poor solvents outside and inside the HSP sphere are plotted as red solid squares and red open squares, respectively. The probe near the center can easily disperse the Si−Ge nanosheets. DMSO was found to be a good solvent in this study.

The HSP values obtained by the HSP sphere method are summarized in Table 1 including the previous data. Note that Si−Ge nanosheet #1, #2, and #3 are based on the data obtained by sedimentation after 2 h, 1 day, and 2 days, respectively. Si nanosheets #1−3 are synthesized from the $Li_{13}Si_4$ system,[11] which is the same synthesis method used for the Si−Ge. In Si nanosheets #1−3, the surface is considered to be terminated with −OH or Si−O−Si because ethanol is used during synthesis.

https://doi.org/10.1021/acsomega.2c01776
ACS Omega 2022, 7, 18834−18839

On the other hand, GeH nanosheets #1−3 are synthesized by exfoliating layered germanene $(GeH)_n$ in each organic solvent, so the surface is considered to be terminated with Ge−H bonds as shown in Scheme 1a. The thickness of the obtained sheet is about 3 nm, the lateral size is also on the microscale, and the size is almost similar for Si, Si−Ge, and Ge nanosheets, which can be explained by the surface termination groups.

The δH (hydrogen bonding term) values for the Si−Ge nanosheets are higher than those for the other nanosheets immediately after dispersion (while the δP values are about the same as those for Si nanosheets), suggesting the presence of a large number of −OH groups (rather than Si═O and Ge═O groups analogous to high-δP carbonyl-groups) on the surface. This may be due to the difference in the surface of the Si and Ge nanosheets dispersed in various probe liquids, where the corresponding Si−H and Ge−H are oxidized by moisture in the reaction system and gradually converted to Si−OH and Ge−OH.

On the other hand, the Si nanosheets were synthesized by dispersing $Li_{13}Si_4$ in ethyl alcohol, which is the same method used for the synthesis of the Si−Ge nanosheets in this study, but the substitution of germanium makes it easier to be oxidized by moisture in the solvent. The δD (London dispersion term) values for the Si−Ge nanosheets also increased with time, as in the case for the Si nanosheets, suggesting that the −OH bonds of the Si−Ge nanosheets gradually shrank and Si−O−Si or Ge−O−Ge bonds were formed. The δD value is dependent on the size of the constituent atoms as well as on the molecular size and the atomic bonding state. Therefore, the Si−Ge nanosheets are considered to have gradually aggregated due to the condensation of the −OH groups.

More precisely, δD is correlated with the polarizability of the functional groups of constituents. The δD and δH values for the Si−Ge nanosheets were significantly larger than those initially calculated for graphene. This was especially true for the δD value for the Si−Ge nanosheets (~26 $[J/cm^3]^{1/2}$), which was extraordinarily large in comparison with those for the common chemical compounds (15−20 $[J/cm^3]^{1/2}$) that are primarily composed of hydrocarbons, oxygen, and nitrogen.

CONCLUSIONS

Si−Ge nanosheets were synthesized, and their dispersions in organic solvents were investigated. For the GeH and Si nanosheets, initially $\delta P > \delta H$. However, with increasing sedimentation time, $\delta H > \delta P$. Since the Si−Ge nanosheets in this study have a large number of −OH groups added to the backbone from the beginning (large δH and large δP, $\delta P < \delta H$), the surface of the sheets was terminated with−OH groups during synthesis. We have identified several organic solvents (DMSO) in which Si−Ge nanosheets can form dispersions with long-term stability. By using solvent properties found in the literature as well as Hansen solubility parameters, we identified a library of organic solvents that disperse Si−Ge nanosheets. This study of dispersion stability of 2D nanomaterials in organic solvents could lead to advances in many functional applications. Thus, HSP is an effective index to determine the surface morphology change of the exfoliated sheets in the liquid phase.

ASSOCIATED CONTENT

Supporting Information

The Supporting Information is available free of charge at https://pubs.acs.org/doi/10.1021/acsomega.2c01776.

XRD patterns for 2 days and 4 months sedimentation and photographs of Si−Ge nanosheets dispersions after 1 day and 2 days of sedimentation; list of probe liquids with their physical properties; and raw data for light intensity after 2 h, 1 day, and 2 days of sedimentation (PDF)

AUTHOR INFORMATION

Corresponding Authors

Hideyuki Nakano − *Toyota Central R&D Labs., Inc., Nagakute, Aichi 480-1192, Japan;* orcid.org/0000-0002-2866-3282; Email: hnakano@mosk.tytlabs.co.jp

Daisuke Nakamura − *Toyota Central R&D Labs., Inc., Nagakute, Aichi 480-1192, Japan;* orcid.org/0000-0002-7808-0528; Email: daisuke@mosk.tytlabs.co.jp

Complete contact information is available at: https://pubs.acs.org/10.1021/acsomega.2c01776

Author Contributions

#H. N. and D. N. contributed equally to this work.

Notes

The authors declare no competing financial interest.

ACKNOWLEDGMENTS

The authors thank Ms. A. Magome for the sample preparations and dispersions.

REFERENCES

(1) Michel, J.; Liu, J.; Kimerling, L. C. High-performance Ge-on-Si photodetectors. *Nat. Photonics* **2010**, *4*, 527−534.

(2) Fang, Y. Y.; Tolle, J.; Tice, J.; Chizmeshya, A. V. G.; Kouvetakis, J.; D'Costa, V. R.; Menéndez, J. Epitaxy-Driven Synthesis of Elemental Ge/Si Strain-Engineered Materials and Device Structures via Designer Molecular Chemistry. *Chem. Mater.* **2007**, *19*, 5910−5925.

(3) Shimura, T.; Ogiwara, S.; Yoshimoto, C.; Hosoi, T.; Watanabe, H. Fabrication of Fully Relaxed SiGe Layers with High Ge Concentration on silicon-on-insulator wafers by rapid melt growth. *Appl. Phys. Express* **2010**, *3*, 105501.

(4) Tice, J. B.; Chizmeshya, A. V. G.; Roucka, R.; Tolle, J.; Cherry, B. R.; Kouvetakis, J. $Cl_nH_{6-n}SiGe$ Compounds for CMOS Compatible Semiconductor Applications: Synthesis and Fundamental Studies. *J. Am. Chem. Soc.* **2007**, *129*, 7950−7960.

(5) Ohshita, J.; Matsuzawa, Y.; Yagami, T.; Adachi, Y.; Sekiguchi, A.; Ohashi, M.; Nakano, H. Photo-energy Transfer in σ-π Conjugated Polysilanes Prepared by Platinum-catalyzed Reactions of Arylacetylenes with Layered Polysilane. *Chem. Lett.* **2020**, *49*, 1174−1177.

(6) Ohshita, J.; Tanaka, Y.; Yamamoto, K.; Kadowaki, H.; Nakashima, M.; Adachi, Y.; Ohashi, M.; Nakano, H. Optical Properties of Silicon Nanosheets Modified with Triphenylamine and Quinoline Units: Charge and Energy Transfer from Conjugated Substituents to the Catenated Silicon Backbone. *J. Phys. Chem. C* **2020**, *124*, 17347−17351.

(7) Nakano, H.; Tanaka, Y.; Yamamoto, K.; Kadowaki, H.; Nakashima, M.; Matsui, T.; Shirai, S.; Ohashi, M.; Ohshita, J. Silicanes Modified by Conjugated Substituents for Optoelectronic Devices. *Adv. Opt. Mater.* **2019**, *7*, 1900696.

(8) Nakano, H.; Ikuno, T. Soft chemical synthesis of silicon nanosheets and their applications. *Appl. Phys. Rev.* **2016**, *3*, No. 040803.

(9) Nakano, H.; Mitsuoka, T.; Harada, M.; Horibuchi, K.; Nozaki, H.; Takahashi, N.; Nonaka, T.; Seno, Y.; Nakamura, H. Soft Synthesis of Single-Crystal Silicon Monolayer Sheets. *Angew. Chem., Int. Ed.* **2006**, *45*, 6303−6306.

(10) Sugiyama, Y.; Okamoto, H.; Mitsuoka, T.; Morikawa, T.; Nakanishi, K.; Ohta, T.; Nakano, H. Synthesis and Optical Property of Monolayer Organosilicon Nanosheets. *J. Am. Chem. Soc.* **2010**, *132*, 5946−5947.

(11) Nakano, H.; Nakamura, D. Hansen Solubility Parameters of Stacked Silicanes Derived from Porous Silicon. *ACS Omega* **2019**, *4*, 11838−11843.
(12) Nakamura, D.; Nakano, H. Liquid-Phase Exfoliation of Germanane Based on Hansen Solubility Parameters. *Chem. Mater.* **2018**, *30*, 5333−5338.
(13) Süß, S.; Sobisch, T.; Peukert, W.; Lerche, D.; Segets, D. Determination of Hansen parameters for particles: A standardized routine based on analytical centrifugation. *Adv. Powder Technol.* **2018**, *29*, 1550−1561.
(14) Takai-Yamashita, C.; Nagamine, H.; Nakashima, Y.; Bo, P.; Fuji, M. Manipulating the chemical affinity and kinetics of 3D silica particle network via the phase-separation technique. *Adv. Powder Technol.* **2018**, *29*, 3062−3069.
(15) Machui, F.; Langner, S.; Zhu, X.; Abbott, S.; Brabec, C. J. Determination of the P3HT:PCBM Solubility Parameters via a Binary Solvent Gradient Method: Impact of Solubility on the Photovoltaic Performance. *Sol. Energy Mater. Sol. Cells* **2012**, *100*, 138−146.
(16) Badia, A.; Cuccia, L.; Demers, L.; Morin, F.; Lennox, R. B. Structure and Dynamics in Alkanethiolate Monolayers Self-Assembled on Gold Nanoparticles: A DSC, FT-IR, and Deuterium NMR Study. *J. Am. Chem. Soc.* **1997**, *119*, 2682−2692.
(17) Nath, S.; Jana, S.; Pradhan, M.; Pal, T. Ligand-Stabilized Metal Nanoparticles in Organic Solvent. *J. Colloid Interface Sci.* **2010**, *341*, 333−352.
(18) Hansen, C. M. *Hansen Solubility Parameters: A User'S Handbook*; CRC Press: Boca Raton, FL, 2007.
(19) Abbott, S.; Hansen, C. M.; Yamamoto, H.; Valpey, R. S. *Hansen solubility parameters in practice, complete with eBook, software and data 4th edition version 4.1*. http://www.hansensolubility.com/ (accessed 18 November 2016).
(20) Nakamura, D.; Shigetoh, K.; Suzumura, A. Tantalum carbide coating via wet powder process: From slurry design to practical process tests. *J. Eur. Ceram. Soc.* **2017**, *37*, 1175−1185.
(21) Nakamura, D.; Hirano, M.; Ohta, R. Nontoxic organic solvents identified using an a priori approach with Hansen solubility parameters. *Chem. Commun.* **2017**, *53*, 4096−4099.
(22) Lang, J.; Ding, B.; Zhang, S.; Su, H.; Ge, B.; Qi, L.; Gao, H.; Li, X.; Li, Q.; Wu, H. Scalable Synthesis of 2D Si Nanosheets. *Adv. Mater.* **2017**, *29*, 1701777.
(23) Yaokawa, R.; Nakano, H.; Ohashi, M. Growth of $CaSi_2$ single-phase polycrystalline ingots using the phase relationship between $CaSi_2$ and associated phases. *Acta Mater.* **2014**, *81*, 41−49.
(24) Shin, H. K.; Lockwood, D. J.; Baribeau, J.-M. Strain in coherent-wave SiGe/Si superlattices. *Solid State Commun.* **2000**, *114*, 505−510.
(25) Tang, Y. S.; Sotomayer Torres, C. M.; Dietrich, B.; Kessinger, W.; Whall, T. E.; Parker, E. H. C. Raman spectroscopy of dry etched Si—$Si_{1-x}Ge_x$ quantum dots. *Solid State Commun.* **1995**, *94*, 369−372.
(26) Talochkin, A. B.; Markov, V. A.; Suprun, S. P.; Nikiforov, A. I. Raman scattering of light by optical phonons in Si-Ge-Si structures with quantum dots. *JETP Lett.* **1996**, *64*, 219−224.

https://doi.org/10.1021/acsomega.2c01776
ACS Omega 2022, 7, 18834−18839